Assessing Cyclone YAAS's Induced Impact on Vegetation Using Multiple Indices: A Case Study on Assasuni Upazila of Bangladesh

Md *Nahid* Ferdous [1*] and Md. *Manjur* Morshed [2]

[1] Institute of Disaster Management, Khulna University of Engineering & Technology
[2] Department of Urban and Regional Planning, Khulna University of Engineering & Technology

Abstract. Tropical cyclones are the most destructive natural disaster, resulting in massive damage to vegetation, infrastructure, and livelihoods. Due to unique geographical location, Bangladesh's coastal area often experiences the devastating effects of the natural disaster. This study assesses the impact of cyclone YAAS on vegetation in May 2021. Three indices (DVDI, DNDVI, and DEVI) were used to evaluate the vegetation damage in Assasuni Upazila (Bangladesh). Sentinel-2A satellite imagery was processed via the Google Earth Engine (GEE) platform. The study found that DNDVI, with an AUC of 0.833, is the most accurate index for detecting vegetation damage after a cyclone, surpassing DEVI and DVDI. DVDI shows the highest severe damage (31.92%) compared to other indices. The study also examined how six topographic factors relate to the most effective damage index using both linear and nonlinear methods. Elevation showed a moderate correlation (R^2 = 0.3993), indicating that areas at higher elevations tend to experience less damage, likely due to reduced exposure to storm surges. Storm surge height showed the strongest polynomial relationship (R^2 = 0.5708). The study's findings can enhance coastal resilience against future cyclones by implementing land use planning and restoring natural barriers, thereby enhancing global disaster preparedness and climate adaptation efforts.

Introduction

Natural disasters have increased globally, with economic losses arising from USD 14 billion in 1985 to over USD 140 billion in 2014 [1]. Asia has been the most affected, with 89% of the global disaster-impacted population between 1975 and 2006 [2]. Among natural disasters, tropical cyclones are particularly destructive, not only causing fatalities and economic losses but also damaging vegetation. Bangladesh, due to its geographic location, is highly vulnerable to disasters such as cyclones, floods, and landslides, with cyclones being the most devastating. These cyclones typically make landfall in April–May or October–November, severely affecting coastal regions [3]. According to the statistics of Department of Disaster Management (DDM) Bangladesh has experienced 508 cyclones in the past century, with 17% hitting Bangladesh [4]. Cyclone YAAS made landfall on May 26, 2021, damaging about 12,150 hectares of cropland, including rice and vegetables, out of 210,135 hectares in total, causing significant agricultural loss [5]. Remote sensing is a highly effective method for assessing vegetation damage from large-scale natural disasters. By analysing changes in vegetation indices (DEVI, DNDVI) from pre- and post-disaster imagery, researchers can accurately measure damage at the pixel level, as demonstrated in

* Corresponding author: nahidferdous103@gmail.com

numerous studies. However, NDVI and EVI values are sensitive to ecological conditions, causing a 49% drop after Hurricane Katrina [6]. To address this, Di et al. (2018) [7] introduced the Disaster Vegetation Damage Index (DVDI), which normalizes vegetation changes against historical variability. Despite its potential, DVDI lacks extensive validation across various disaster types. Topographic parameters like elevation, slope, wind speed, and soil moisture significantly influence vegetation damage. These factors affect microclimatic conditions, water drainage, and wind exposure, shaping vegetation vulnerability to cyclonic events [8]. However, topographic influences are often overlooked in post-disaster vegetation assessments. Integrating these variables into damage models can improve risk assessments and mitigation strategies. Google Earth Engine (GEE) is a cloud-based platform that efficiently processes large volumes of satellite data for analysis. It supports various datasets, including Sentinel, and is used for forest monitoring, flood mapping, and land use studies. The study aims to identify the most effective vegetation damage (VD) evaluating cyclones and explore factors influencing vegetation damage, aiding in disaster management and resilience building along Bangladesh's southwestern coast.

Study Area

The study area (Fig.1) in Assasuni Upazila, Satkhira district, spans 378.28 square kilometers and has a population of 292,292 with a density of 726.44 per sq km. The primary occupations are agriculture and fishing. On May 26, 2021, cyclone YAAS made landfall, causing extensive damage and significant losses, breaching polders and flooding agricultural land [9].

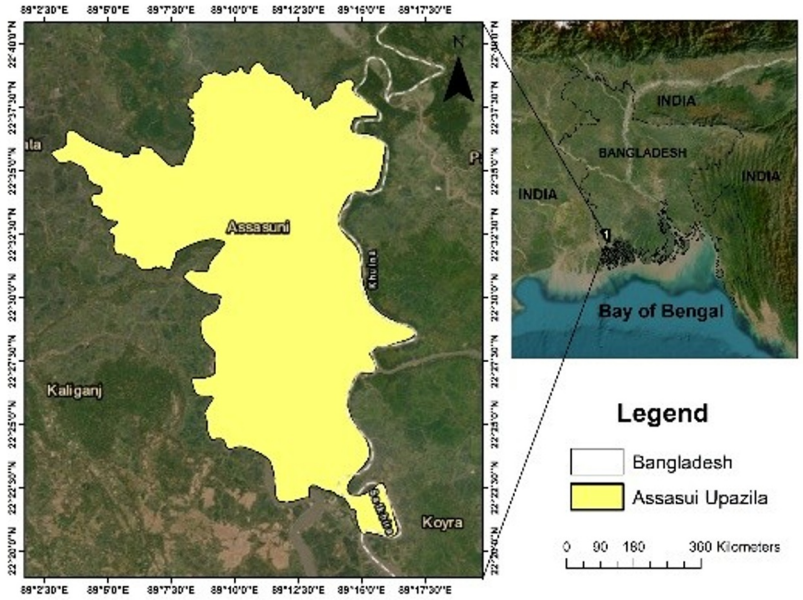

Fig. 1. Study Area

Methods

Satellite images and preprocessing

In this study, all satellite imagery was acquired and processed through the Google Earth Engine (GEE) platform. We used the Sentinel-2A satellite imagery dataset, which has been freely available since 2015 and provides global coverage with a spatial resolution of 10 meters. Its accessibility and high-resolution data have made it a popular choice in remote

sensing research, supporting a wide range of geospatial applications such as land cover change detection, agricultural monitoring, land use mapping, and more [8].

DVDI

Disaster Vegetation Damage Index (DVDI) is applied to measure post-disaster vegetation damage [8]. It is calculated according to Eq. (1).

$$DVDI = mVCI_a - mVCI_b \quad (1)$$

DNDVI and DEVI

DNDVI (Differenced Normalized Difference Vegetation Index). is the commonly used index for vegetation damage assessment [8] and can be computed using Eq. (2).

$$DNDVI = \frac{NDVIa - NDVIb}{NDVIb} \quad (2)$$

The Difference in enhanced vegetation index (DEVI) is a widely used indicator for assessing vegetation damage [8]. It is derived using surface reflectance values from the red, near-infrared, and blue spectral bands, specifically corresponding to Bands 2, 4, and 8 of the Sentinel-2A satellite. The index is computed using Equation (3), building upon the Enhanced Vegetation Index (EVI) to better capture vegetation changes related to disaster impacts.

$$DEVI = EVI_a - EVI_b \quad (3)$$

Topographic parameters

The study examined the correlation between vegetation damage and landscape topographic features and cyclone trajectory. Key factors included elevation, slope, soil moisture, storm surge height, distance from the cyclone path, and wind speed. Data from the Bangladesh Meteorological Department, NASA Shuttle Radar Topography Mission, and SMAP Enhanced L3 Radiometer Global and Polar Grid Daily Version 3 datasets were used. The spatial distribution of vegetation index value was analysed, and linear and nonlinear regression analyses were performed to assess the influence of topography on vegetation damage**.**

Accuracy assessment

The accuracy assessment involved randomly selected samples from damage estimation results, visually verified using high-resolution imagery from Google Earth pro, and performance assessed using ROC curves and AUC values. The AUC ranges from 0 to 1, indicating perfect accuracy, random guessing, or poor performance [10].

Result

Validation

Fig.2. presents ROC curves for three vegetation damage assessment models (DVDI, DNDVI, and DEVI) based on satellite imagery after a cyclone. The DNDVI model showed

the highest accuracy with an AUC of 0.833, followed by DEVI (0.767) and DVDI (0.633). The ROC curve analysis indicates that DNDVI had the strongest predictive performance, positioned closest to the top-left corner of the plot. These findings demonstrate that different vegetation indices vary in effectiveness, highlighting the need to choose appropriate indices for accurate post-cyclone vegetation damage assessment crucial for disaster response and recovery in vulnerable Coastal regions.

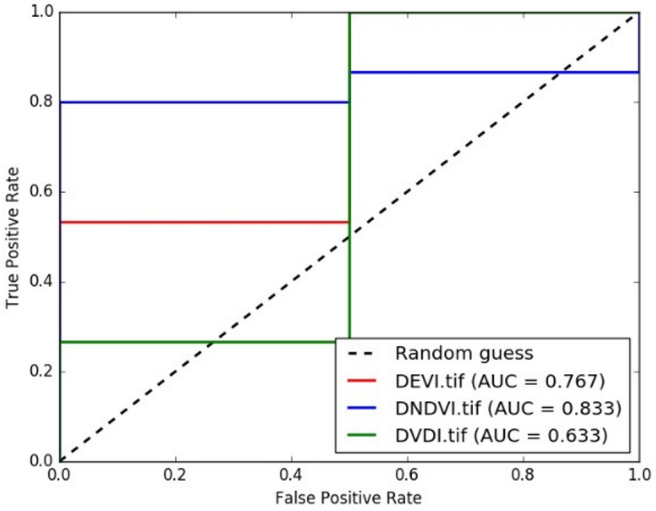

Fig .2. Accuracy Assessment of the Indices (DEVI, DNDVI, DVDI)

Visualizing DEVI, DNDVI and DVDI

Fig. 3 displays the spatial pattern of vegetation damage detected by the DEVI. Most of the western, southern, and central regions appear as 'no damage' zones, indicating vegetation resilience. In contrast, moderate to severe damage is mainly found in the eastern and southeastern areas, likely due to tidal surges or low elevation. Fig.4 illustrates the spatial distribution of vegetation damage based on DNDVI analysis. Most areas are classified as ‘no damage’ (green), indicating minimal vegetation change, predominantly in the western, north central, and parts of the southeastern regions. ‘Moderate damage’ zones (yellow) are scattered throughout the landscape, with notable concentrations in the northwestern, central, and southeastern areas. Clusters of ‘severe damage’ (red) are mainly found in the eastern and southern parts of the Upazila. This distribution highlights spatial variability in cyclone impact, emphasizing the usefulness of DNDVI in detecting differing levels of vegetation damage. Fig.5 displays the spatial distribution of vegetation damage using the Disaster Vegetation Damage Index (DVDI), categorized into 'no damage' (green), 'moderate damage' (yellow), and 'severe damage' (red). Compared to previous indices, this map reveals a greater density and broader spread of damaged areas. Severe damage is widespread across the central, western, and northwestern regions, indicating extensive vegetation loss. Moderate damage zones are more continuous and expansive, forming belts between the most and least affected areas. While some 'no damage' areas remain, particularly in the southeastern and northeastern parts, they occupy a much smaller portion of the landscape.

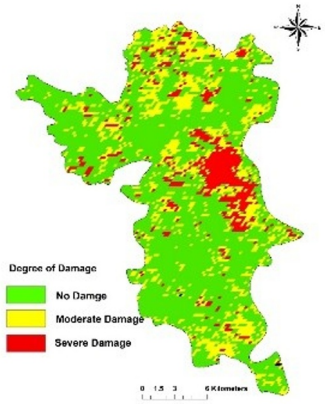

Fig.3. Difference in enhanced vegetation index (DEVI)

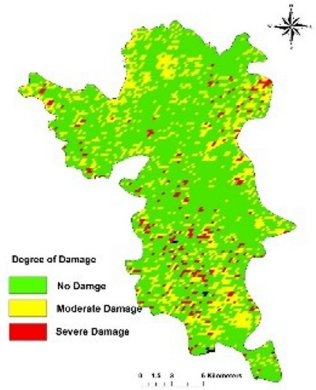

Fig.4. DNDVI (Differenced Normalized Difference Vegetation Index).

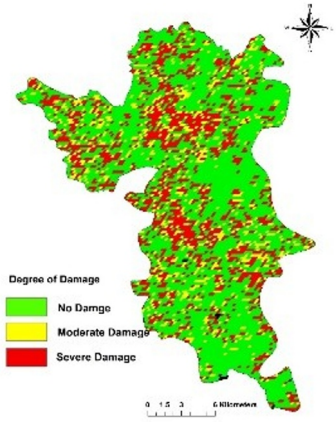

Fig.5. Disaster Vegetation Damage Index (DVDI)

Quantitative assessment

Table 1. Area Calculation of Damage Class

Damage Class	DEVI		DNDVI		DVDI	
	Area	%	Area	%	Area	%
No Damage	202.67	53.58%	213.97	56.56%	188.97	49.96%
Moderate Damage	95.81	25.33%	106.16	28.06%	68.55	18.12%
Sever Damage	79.80	21.10%	58.15	15.37%	120.76	31.92%
Total	378.28	100.00%	378.28	100.00%	378.28	100.00%

Table 1 provides a comparative analysis of vegetation damage using three remote sensing indices: DEVI (Difference in enhanced vegetation index), DNDVI (Differenced Normalized Difference Vegetation Index), and DVDI (Disaster Vegetation Damage Index). Each index categorizes the area into No Damage, Moderate Damage, and Severe Damage. According to DEVI, the majority of the area (53.58%) showed no vegetation damage, with moderate and severe damage covering 25.33% and 21.10%, respectively. The DNDVI results are similar, indicating 56.56% undamaged area, 28.06% moderate damage, and 15.37% severe damage. In contrast, DVDI, which is specifically designed for disaster assessment, reveals a stronger impact: only 49.96% of the area remained undamaged, while severe damage affected 31.92% and moderate damage 18.12%. These findings highlight differences in damage detection among the indices, with DVDI identifying a greater extent of severe vegetation damage, suggesting it may be more effective in detecting post-disaster vegetation stress.

Topographic parameter influences on vegetation damage

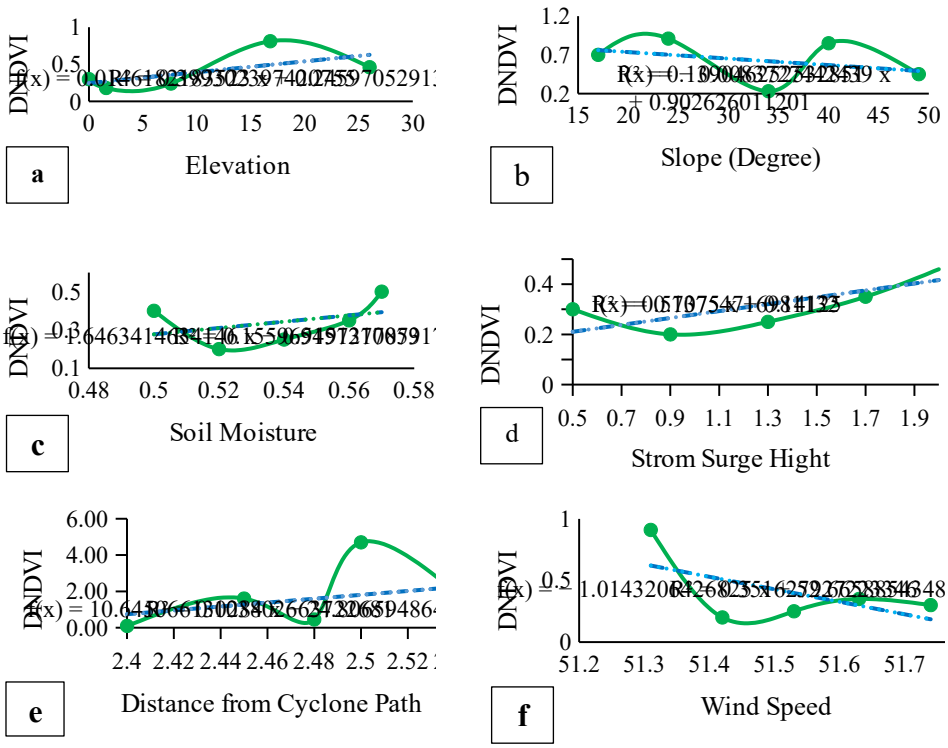

Fig. 6. Relation between the topographical factors and vegetation damage index

Figure 6 explores the relationship between DNDVI and six topographic and environmental factors. Elevation (Fig.6a) shows a moderate positive correlation (R^2 = 0.3993), indicating healthier vegetation at higher altitudes. Slope (Fig.6b) has a weak negative correlation (R^2 = 0.139), with DNDVI slightly decreasing as slope increases. Soil moisture (Fig.6c) exhibits a weak positive correlation (R^2 = 0.156), forming a U-shaped trend where DNDVI initially

declines and then rises. Storm surge height ((Fig.6d)) demonstrates a moderate correlation ($R^2 = 0.5708$), with DNDVI decreasing and then increasing beyond a certain surge height. Distance from the cyclone path (Fig.6e) shows a weak correlation ($R^2 = 0.1038$), with DNDVI peaking around 2.5 km before declining. Wind speed (Fig.6f) has a moderate negative correlation ($R^2 = 0.3516$), where DNDVI decreases sharply with increasing wind speed. Overall, these results highlight that elevation and storm surge height have the strongest influence on post-cyclone vegetation damage among the factors analyzed.

Discussion

This study compared three methods for assessing cyclone-induced vegetation damage and found that DNDVI was the most accurate (AUC = 0.83) (Fig.2), followed by DEVI, while DVDI showed the lowest performance. DNDVI and DEVI were also easier to implement, requiring only two satellite images and minimal processing, supporting earlier findings by Chen et al. (2022) [8] on their effectiveness for rapid assessment of vegetation damage. The use of Google Earth Engine (GEE) facilitated data access and processing but may pose challenges for users unfamiliar with coding or without stable internet, in contrast to GUI-based tools like ArcGIS or QGIS. As shown in Table 1, vegetation damage estimates were 46.43% (DEVI), 43.43% (DNDVI), and 50.04% (DVDI), while official estimates from the Department of Agricultural Extension (DAE) [5] reported 39% of vegetation was damaged during Cyclone YAAS. DVDI's higher estimate may result from limitations in Sentinel-2A's 10-day revisit period and its reliance on historical baseline data, which may reduce accuracy if temporal coverage is insufficient. Furthermore, DVDI's use of high-resolution imagery (10 m) could lead to overestimations, unlike coarser-resolution sensors like MODIS (250 m), which have been found to yield more balanced results in previous studies [7,8].

This study examined how topographic and environmental factors influence vegetation damage from cyclones, building on prior research [11]. Key variables elevation (Fig.6a), slope (Fig.6b), soil moisture (Fig.6c), storm surge height (Fig.6d), proximity to the cyclone path (Fig.6e) and wind speed (Fig.6f), were identified as contributors to vegetation vulnerability. Results showed that elevation (Fig.6a) had a moderate positive correlation with DNDVI ($R^2 = 0.3993$), suggesting reduced damage at higher elevations, consistent with Zhang et al. (2021) [12]. Slope (Fig.6b) showed a weak negative correlation ($R^2 = 0.139$), possibly due to erosion, though nonlinear patterns suggest intermediate slopes may offer some resilience. Soil moisture (Fig.6c) followed a U-shaped relationship ($R^2 = 0.156$), with both low and high moisture levels linked to reduced vegetation health, aligning with findings from Yu et al. (2024) [13]. Storm surge height (Fig.6d) showed the strongest correlation ($R^2 = 0.5708$), with a threshold-like effect and offering same finding with the study conducted by Niwa et al., (2023) [14]. Distance from the cyclone path (Fig.6e) had a weak correlation ($R^2 = 0.1038$), while wind speed (Fig.6f) showed a moderate negative correlation ($R^2 = 0.3516$), confirming that stronger winds increase damage, as reported by Liu et al. (2024) [15]. These findings underscore the value of integrating multiple biophysical variables in cyclone damage modeling and highlight the need for future studies to explore how revisit frequency and spatial resolution influence the accuracy of indices like DVDI, especially in the context of other hazards such as droughts, forest fires, and landslides.

Conclusion

This study emphasizes the practical benefits of using DNDVI for rapid post-cyclone vegetation damage assessment due to its simplicity, requiring only pre- and post-event

imagery with minimal processing. Its strong performance reinforcing its utility for operational disaster monitoring. While DVDI captured more extensive severe damage, this may reflect limitations in Sentinel-2A's revisit frequency and the dependence on historical vegetation baselines, which can introduce uncertainty in fast-changing landscapes. Furthermore, comparisons with ground data from the Department of Agricultural Extension revealed that satellite-based damage estimates were generally higher, indicating that remote sensing can capture subtle or widespread impacts that may be missed in field reports. By integrating environmental and topographic variables such as elevation, slope, wind speed, and storm surge the study provides insight into the spatial drivers of damage, supporting more targeted recovery planning. The use of cloud-based platforms like Google Earth Engine enabled large-scale processing, though barriers remain unfamiliar for users with code-based tools. A limitation of this study is the use of optical satellite data, which can be affected by clouds or haze. Future research should focus on refining these methods with SAR data and testing their adaptability in other disaster contexts, such as droughts or wildfires, to further advance remote sensing applications in climate resilience and emergency response planning.

References

1. B. H. Nam, S. Choi, T. Copeland, and Y. J. Kim, "Social Vulnerability and Geohazards: Review and Implications," in Advances in Natural and Technological Hazards Research, vol. 51, Cham: Springer, pp. 3–37 (2023). doi: 10.1007/978-3-031-24541-1_1.
2. Asian Development Bank, ADB Climate Change Programs: Facilitating Integrated Solutions in Asia and the Pacific. Mandaluyong City, Philippines: Asian Development Bank, 2010. [Online]. Available: http://www.indiaenvironmentportal.org.in/files/adb-climate-change-programs-brochure.pdf [Accessed: May 3, 2025].
3. H. Irin and M. Ashekur, "Cyclone and Bangladesh: A Historical and Environmental Overview from 1582 to 2020," International Medical Journal, vol. 25, no. 06, pp. 2595–2614, (2020).
4. Department of Disaster Management, Bangladesh (DDM), Department of Disaster Management. [Online]. Available: https://ddm.gov.bd/. [Accessed: Apr. 25, 2025].
5. Department of Agricultural Extension, Bangladesh (DAE), Department of Agricultural Extension. [Online]. Available: https://dae.gov.bd/. [Accessed: Apr. 27, 2025].
6. J. C. Rodgers, A. W. Murrah, and W. H. Cooke, "The impact of Hurricane Katrina on the coastal vegetation of the Weeks Bay Reserve, Alabama from NDVI data," Estuaries and Coasts, vol. 32, pp. 496–507, (2009).
7. L. Di, E. Yu, R. Shrestha, and L. Lin, "DVDI: A new remotely sensed index for measuring vegetation damage caused by natural disasters," in Proc. Int. Geosci. Remote Sens. Symp. (IGARSS), Jul. (2018), pp. 9067–9069. doi: 10.1109/IGARSS.2018.8518022.
8. X. Chen et al., "Post-typhoon forest damage estimation using multiple vegetation indices and machine learning models," Weather and Climate Extremes, vol. 38, p. 100494, (2022). doi: 10.1016/J.WACE.2022.100494.
9. R. Subhani, S. E. Saqib, M. A. Rahman, M. M. Ahmad, and S. Pradit, "Impact of Cyclone YAAS 2021 aggravated by COVID-19 pandemic in the southwest coastal zone of Bangladesh," Sustainability, vol. 13, no. 23, p. 13324, (2021). doi: 10.3390/SU132313324.

10. A. M. Carrington et al., "Deep ROC analysis and AUC as balanced average accuracy, for improved classifier selection, audit and explanation," IEEE Trans. Pattern Anal. Mach. Intell., vol. 45, no. 1, pp. 329–341, (2022). doi: 10.1109/TPAMI.2022.3153406.
11. Y. Feng, R. I. Negron-Juárez, and J. Q. Chambers, "Remote sensing and statistical analysis of the effects of Hurricane María on the forests of Puerto Rico," Remote Sens. Environ., vol. 247, p. 111940, (2020). doi: 10.1016/j.rse.2020.111940.
12. Q. Zhang, Z. Wu, and P. Tarolli, "Investigating the role of green infrastructure on urban waterlogging: Evidence from metropolitan coastal cities," Remote Sens., vol. 13, no. 12, p. 2341, (2021).
13. Y. Yu et al., "Disturbance types play a key role in post-disturbance vegetation recovery in boreal forests of Northeast China," Ecol. Indic., vol. 168, p. 112745, (2024).
14. H. Niwa, M. Kamada, S. Morisada, and M. Ogawa, "Assessing the impact of storm surge flooding on coastal pine forests using a vegetation index," Landscape and Ecological Engineering, vol. 19, no. 1, pp. 151–159, (2023).
15. Y. Liu, F. Wang, F. Ji, L. Zhang, J. Zhao, C. Zheng, and J. Chen, "The response characteristics and stability evaluation of vegetated slope under strong wind," Scientific Reports, vol. 14, no. 1, p. 29045, (2024).